

Investigation of the glider load spectra

Mirosław Rodzewicz
Warsaw University of Technology
Nowowiejska 24, 00-665 Warsaw, Poland
miro@meil.pw.edu.pl

Presented at the XXVIII OSTIV Congress, Eskilstuna, Sweden, 8-15 June 2006

Abstract

The paper presents the results of work aimed at the investigation of the load spectra. The investigated object was a PW-5 glider equipped with a wing-spar root deflection measurement and accelerometer. The records of the loads were made during several flight-tasks: thermal flying, soaring, wave-flying and aerobatics. The results of the investigation are presented as load spectra in the form of the Markov-matrix. A second subject concerns the extrapolation of the load spectrum recorded during investigations for extended-time operation. The third problem reported is the comparison of the calculated damage accumulation effect induced by different load spectra.

Introduction

Information about the load spectrum (LS) is necessary for estimation of a glider's operational life. As it is well known, the LS contains data on the number of load cycles at a given range of load factor variation. Such information is crucially important for the glider certification procedure

Load spectrum evaluation

The first step for the LS estimation is load recording during the glider's operation. In the case of the PW-5 glider, designed at the Warsaw University of Technology, the system for the LS data collection is shown in the Fig. 1.¹ The system consists of the following three basic elements:

- *Electronic accelerometer*
- *Wing spar root deflection sensor*
- *Digital data recorder*

Figure 2 presents the sample time-courses of two signals recorded during a short flight (aerodrome circle) consisting of: winch towing, period of smooth gliding and some aerobatic evolutions. The upper signal u comes from the wing spar root deflection sensor, while the lower signal n_z comes from the accelerometer.

Those signals can be correlated by presenting them in the same diagram (the accelerometer signal marked on the vertical axis and the signal from the wing spar root deflection sensor on the horizontal axis). It can be clearly seen that in some areas of the diagram (Fig. 3) those two signals are correlated while in the other areas they are not correlated.

More detailed analysis of Fig. 3 shows us that the first non-correlated zone is associated with the period of winch launching and the other one is associated with the ground operations, especially the take-off and landing run. During a free flight, it can be observed the full correlation between the signals, and the correlation formula is linear.

The best way for load spectrum evaluation consists of using the Markov transfer matrix MM . This method was elaborated by German scientists² (Fig. 4).

The Markov matrix used for the LS is a square array, comprising 32 x 32 cells. The cell with the index i,j contains the number of load changes from the i -th level to the j -th level. The diagonal containing the cells with the index $i=j$ is called „0-Diagonal” and is eliminated. To apply this matrix, the signal recorded during the flight should be filtered and transferred from the form of a 2-column array (i.e. Time and Signal Value according to a sampling frequency of the digital recorder) to the form where the signal is represented only by the sequence of Local Extremes. Following the Local Extremes sequence for the whole flight course, it is possible to fill-up the Markov matrix which, then, covers the whole information about the load spectrum during the flight.

An example of such a matrix is shown in Fig. 5. In this sample case, the signal from the wing spar root deflection sensor (recalculated on the Load Levels scale) from Fig. 2 was used here as the input-data.

Other time-courses of the load signals, registered in different kinds of flights underwent the same procedure. The output is shown in the Fig. 6 in the form of sample Markov matrices determined for Thermal flight, Soaring flight, Wave flight and Aerobatic flight. The light color indicates the active zone of the Markov matrix, i.e. the square which is the envelope of rows and columns containing at least one signal change. The dark color indicates the zone of small load variations near $n_z = 1$. The following features are noted from Fig. 6:

- It can be seen that, as expected, the largest active zone of the matrix is produced during the Aerobatic flight.
- The Wave flight produces also a large active zone, but it is due to the rotors influence mainly in the first stage of the flight. Later in the flight it is very smooth and the number of load changes increases mainly near the dark zone.
- The smallest active zone was produced during the Thermal flight. In this case it was quite a smooth flight – just a recreation flight over the airfield. During cross country flights this active zone is larger. From author's experience, the

difference between the active areas of the matrix concerning Thermal flight or Soaring flight is not large.

The Markov matrix creates the bases for easy processing of the load spectra. Having the set of Markov matrixes obtained for several flights or several flight missions, it is possible to produce a new matrix as a sum of all single matrices. This matrix presents the cumulative load spectrum for certain operation time (i.e. the total number of flight hours spent during the LS recording session).

The load spectrum in the form of a Markov matrix is very useful. For example, it is easy to transfer this form of the LS to one of the traditional (i.e. incremental) forms, represented by the Δn_z and the cumulative number of occurrences. Before this operation it is necessary to apply the Rainflow Counting Algorithm when the Markov matrix is calculated.³

Sequentially eliminating the values along the diagonal lines starting from the first pair of lines close to the „0-Diagonal”, and counting a sum of the values in the remaining cells of the matrix, it is possible to obtain the number of occurrences for different values of the Load Level increment ΔLL . The result of this operation is shown in the table situated in the Fig. 7. Presented in the table are the numbers of occurrences for ΔLL equal to at least 1, or at least 2 and so on. In the case considered here, the absolute value of the ΔLL was taken into account. This means that the concept of a symmetrical model of the load spectrum is investigated here.

The table in Fig. 7 contains also the values of Δn_z calculated for given values of ΔLL . It allows us to present the measured load spectrum in the traditional form i.e. Δn_z versus NC_{1h} , where NC_{1h} is the cumulative number of occurrences per hour. Instead of the curve interpolating the Test-Data, it is possible to apply a broken line. This method produces the chart called Kaul's Diagram in Fig. 7, which was used in the past for load spectra calculation.

If the positive and negative values of ΔLL are separated, it is possible to introduce the concept of a asymmetrical model of the load spectrum (Fig. 8). The table in that figure contains the values of numbers of the load changes separately for negative and positive ΔLL (or for the corresponding values of Δn_z). The load spectrum obtained using this method is shown in the chart in Fig. 8. As it can be seen, the left and right branches of the chart are not exactly the same. This means that taking into consideration the absolute values of the ΔLL , the resulting load spectrum is more conservative and overloads the construction during fatigue tests.

Load spectrum extrapolation

When the load spectrum for a certain time of operation is obtained, the main problem consists in extrapolation of this spectrum for the Modeled Period of Operation - MP ; (in general $MP = 1000$ flight hours). The extrapolation may be achieved using several methods. The first method is a statistical analysis of the cumulative occurrences per hour NC_{1h} at a given ΔLL performed on the series of recorded load

spectra. An example of this analysis, conducted for 8 thermal flights (where the total operation time was 914 minutes in the air), is presented in Fig. 9 the chart containing two curves. The lower curve represents the mean value of the $NC_{1h,m}$. The upper curve represents the upper values of the cumulative number of load changes per hour $NC_{1h,up}$. This curve is generated by adding 3σ (three standard deviations) to the mean value for each ΔLL . The curves obtained in this way create a basis for load spectra extrapolation.

In the case of an incremental load spectrum, two concepts of the extrapolation were considered:

- Method I: Expanding the range of ΔLL for Test-Data mean values up to the limit specified by the rules for a given type of the glider (Fig. 10). In this case, the values at the vertical axis are calculated using the formula given in the upper chart.
- Method II: Extrapolating the Test-Data range by means of the curve calculated from the Test-Data approximation formula (Fig. 11). This formula is produced using the data formed by the pair of numbers: the ΔLL (or Δn_z) and by the $NC_{1h,up}$ multiplied by 1000; (as assumed here the Modeled Period $MP = 1000$ h).

The application of the Markov matrix to the load spectrum presentation allows for extrapolation of the Test-Data for the Modeled Period of operation, using stochastic methods (Method III). Such an extrapolation was made by the author using a special computer program. The idea of extrapolating procedure is as follows. Suppose that our interest is focused on the standard flight mission (with a recurrent scenario), for example the Thermal flying over the airfield (without any non-standard behavior, i.e. intentional aerobatics). Suppose that we have recorded the loads during such a flight and obtained the Markov matrix which is treated as the input-data matrix. If there are a number of occurrences in the cell MM_{ij} , then in the next flights we may expect that this number of occurrences will be redistributed around the cell MM_{ij} according to the 2-dimensional Gauss distribution (Fig. 12).

This redistribution takes place for each cell of the data-input matrix and can be simulated numerically. As a temporary-output we obtain a matrix of the values calculated as superposition of all redistributions. This process may be repeated several times. At the end, we obtain an output-matrix with the simulated load spectrum for other flights. The process is stochastic, so every output is different.

Of course in the case of single flights, the probability is low that the simulated load spectrum will be exactly the same as any spectrum measured in flight. But in the case when the input-matrix is a cumulative matrix for a series of flights, and we sum the outputs from the simulation process up to the Modeled Period of Operation, the probability is high that the final result will be similar to the spectrum measured for the same period and depends on the cumulative number of flight-hours for the input-matrix.

As an example of such an extrapolation method, three simulations were made. It was assumed in the program that redistribution of the cell MM_{ij} value can be performed in the

range covering ± 2 cells (in rows and in columns) of the Markov matrix.

Three quasi-Gaussian probability distributions were applied (Fig. 13). The algorithm of redistribution was repeated 20 times for a single program run. As a result, three output matrices were obtained. Figure 14 presents the input-matrix and one of the output matrices. It can be seen that the active zone of the output-matrix increased, as compared to the input-matrix. The cumulative number of occurrences also increased (approximately linearly as the simulated operation time passed). Together with the MMs, the 3-D images of values distributions are presented in the input and output matrices. When applying a linear scale for the vertical axis, almost the same shape of 3-D images resulted (the number of occurrences differed only). The differences become visible after changing the linear scale into a logarithmic scale, and such images are displayed in Fig. 14.

Figure 15 presents the comparison between the load spectra for 1000 hours of operation obtained using different extrapolation methods. This is a result of the Rainflow Counting Algorithm application to the data written as the Markov matrices.

The load spectrum used for PW-5 glider fatigue tests (application of the Stafiej LS evaluation method⁴) and the load-increments derived from the standard load spectrum Kosmos 2 are used as the reference. *It is very important to emphasize here, that both these reference spectra cover all flight missions - not only Thermal flights!*

It can be seen that the biggest number of load changes for each ΔLL -value results from Method I. Method II generates the spectrum, for which the Stafiej-spectrum looks as a step-envelope. The results of Method III are the lowest, but the number of loads (starting from $\Delta LL = 7$) increases as the probability distribution in the “MM-redistribution program” becomes more flat.

Load spectrum and fatigue effect

The comparison between load spectra using only the cumulative number of occurrences is insufficient. Much more useful is a comparison using the fatigue damage accumulation CD . The basic theory here is the Palmgren-Miner hypothesis. The Palmgren-Miner formula adapted for the Markov matrix applications is written below.

$$CD = \sum_{i=1}^{32} \sum_{j=1}^{32} D_{i,j} = \sum_{i=1}^{32} \sum_{j=1}^{32} \frac{n_{i,j}}{N_{i,j}} = 1$$

Instead of load cycles, we now have the load changes (load increments). *One occurrence* of load change between the levels i and j plus *one occurrence* of load change between the levels j and level i produce *one load cycle*. The symbol N in the above formula indicates the number of load changes to failure, while the symbol n indicates the number of loads changes in the spectrum.

For damage calculations, we need information about the values of N . This is a serious problem because the data are difficult to obtain. One of the best ways for storing the data is the Haigh diagram. Figure 16 presents the diagram published by Kensche for the composite used for the wing spar web.⁵ The dark color indicates the useful zone of this diagram when the wing spar web is calculated for the stress-level limit in terms of the factor $K_{\sigma l} = 16 \text{ km}^{6,7}$.

This diagram was used for calculation of damages produced by different load spectra. For this purpose a special array was created (Fig. 17) containing the damage D_{ij} values for the unitary Markov matrix (all cell values equal 1, except for „0-Diagonal”).

As it can be seen in Fig. 17 the damage value D_{ij} depends strongly on the position of the cell in the Markov matrix. In the linear scale, only values in the cells situated far enough from the „0-Diagonal” are visible in the bar-chart. Application of the logarithmic scale reveals that the difference between D -values for near the „0-Diagonal” cells and the cell $MM_{3,31}$ or $MM_{31,3}$ is about 10 orders.

That is why the positions of the cells in the matrix containing the LS is important. Even if the number of load changes in the cells near the „0-Diagonal” is relatively high, those cells do not produce significant values of damage, as compared with the cells containing small numbers but situated far from „0-Diagonal”. That is also the reason why in the spectrum Kosmos 2, the values in 4 cells under and over the „0-Diagonal” are neglected.

Having the array of damage D_{ij} values for the unitary Markov matrix it is very easy to calculate the accumulated damage CD for the load spectra written as a Markov matrix.

The procedure consists of the following two steps:

1. Multiply the values MM_{ij} and D_{ij} in the whole range of indices i, j variation;
2. Sum up all results.

In the case of the traditional (incremental) form of the load spectrum, it is necessary to write this spectrum into the Markov matrix. As in the incremental kind of spectrum, the information about reference level of loads is lost during the spectrum creation. Thus, this operation may be performed only in an approximate way.

The Fig. 18 displays the algorithm of the method applied by the author:

1. Having the load spectrum curve, write it as the step-wise spectrum.
2. For each stair level, find the appropriate diagonal line in the Markov matrix.
3. Distribute the total number of load changes for each step along the diagonal line according the Gauss distribution.

Figure 19 presents the comparison between damage accumulations for the different methods of extrapolation. The analysis is made for the wing spar web based on the High diagram presented in the Fig. 16. As a reference, bars show the results calculated for reference spectra No 1 and No 2.

Method I produces the most restrictive load spectrum which yields the highest value of damage accumulation.

Method II yields the result which is placed a little bit under the damage accumulation value of Reference LS No 2. It is necessary to emphasize that application of this extrapolation method is hazardous because it is an extended extrapolation and the shape of extrapolation curve strongly depends on the topology of the input-data (see Fig. 11). The solution to this problem would be the pre-specification of certain values at ΔLL_{max} (for example 10^2 load changes).

The results from Method III depend on the assumed probability distribution. Although the results are much lower than those from Methods I and II, it is still a conservative damage accumulation evaluation method. The conservatism of the method is visible in the chart (Fig. 20) presenting the comparison between the following results:

- *Test LS* – the damage accumulation for Test-Data;
- *Prop-Test LS*– the damage accumulation for multiplication of the Test LS value by 65 (i.e. Ratio between a 1000 hours and the total flight-time for the Test-data);
- *Met III-1, Met III-2, Met III-3* - the damage accumulation for Method III with different probability distributions.

Although the number of load changes (accumulated number of occurrences) is highest for *Prop-Test LS*, all results from Method III are much higher than the *Prop_Mag* result. The main problem here is a proper choice of probability distribution. It can be made having a larger Test-Data base.

The last problem is the number of extreme-amplitude load cycles (i.e. cycles between 3-th and 31-st load level) which may be used as some kind of a substitute for the full load spectrum. Calculations were made on the same basis as previously (i.e. the same array of elementary fatigue damages for the unitary Markov matrix derived from the High diagram presented in Fig. 16).

Comparing the damage accumulation for a single extreme-amplitude load cycle with the damage accumulation for two different load spectra, the Adequate Number of Extreme-Amplitude Loads (ANEAL) was calculated.

In case of the Reference LS No 1, the ANEAL = 229 for 1000 operational hours while the number of the highest amplitude loads is 152. It means that only this part of the spectrum, which contains high increments of the loads exerts a decisive influence on the damage accumulation. The comparison of the ANEAL value for 12000 operational hours with the 1-step fatigue test proposed by Kensché⁷ is shown in Fig. 21. The ratio between number of load cycles is here 3,65. This value is a bit more conservative than the scatter factor which should be applied to fatigue calculations in the case when only one specimen is tested. But, the results are intended to apply to whole statistic population of the glider-type.

Figure 22 contains a comparison of damage accumulation for two alternative load-programs for the fatigue tests. In the first case, 10 000 of extreme amplitude cycles (from LL=3 to

LL=31) are considered. Alternatively, in the second case, this load program was divided into two separate block of loads: from LL=3 to LL=19 and from LL=19 to LL=31.

As it can be seen from the bar-diagram in Fig. 22, damage accumulation in the first case is 183 times higher then in the second case. This also means that for the same fatigue effect (i.e. damage accumulation value) the second load-program should be repeated 183 times. Alternatively, the second load-program may be replaced with $2 \cdot 10^4 / 183 = 110$ cycles from LL=3 to LL=31.

Of course, all the presented results strongly depend on the input data (i.e. number of loads to failure in the High diagram) and on the operational range of stress (or strains). In the case of a more flat distribution of the number of loads to failure in the High diagram, this substitution ratio will be different (i.e. the number of extreme-amplitude load cycles will be bigger).

General conclusion

The idea of Kensché concerning glider-structure fatigue tests^{8,9} to substitute certain numbers of the extreme-amplitude load cycles for the whole load spectrum seems to be interesting, safe and reasonable.

Since the results of load spectra investigations for different flight missions depend on several parameters, i.e. weather conditions, pilot's experience, and even on the fact if pilot is aware that the measuring equipment has been installed, the load spectra presented in this paper should be considered as sample ones valid for specific conditions.

References

- ¹Rodzewicz M., Przekop A., "Research of the load spectrum and fatigue tests of the PW-5 World Class glider," *Technical Soaring*, Vol. 24, No. 1, pages 15-19, 2000;
- ²Kossira H., Reinke W., "KoSMOS EIN LASTKOLLEKTIV FÜR LEICHTFLUGZEUGE," *DGLR-Jahrestagung*, Hamburg, DGLR-Jahrbuch I, Bonn 1989
- ³Stafiej W., "Zagadnienia związane z programowaniem widma obciążeń eksploatacyjnych szybowców kompozytowych," *Zeszyty Naukowe Politechniki Rzeszowskiej*, Nr 29, Rzeszów 1987
- ⁴Kensché Chr. W., "Proposal for a certification procedure of extended sailplane lifetime," *Technical Soaring*, Vol. 26, No 2, April 2002
- ⁵*Dimensioniren von Bauteilen aus GFK VDI-2013*, VEREIN DEUTSCHER INGENIEURE, Jan 1970
- ⁶*Dimensionierungsrichtwerte für den Segel- und Motorsegelflugzeugbau*, IDAFLIEG, März 1988
- ⁷Kensché Chr. W., "Influence of Composite Fatigue Properties on Lifetime Predictions of Sailplanes," *Technical Soaring*, Vol. 19, No.3, 1995
- ⁸Rychlik I., "A new definition of the Rainflow Cycle Counting Method," *International J. Fatigue* 9, pp 119 – 121, 1987
- ⁹Waibel G., Schleicher A., "Safe life substantiation for a FRP-sailplane," *Technical Soaring*, Vol. 26, No. 2, April 2002

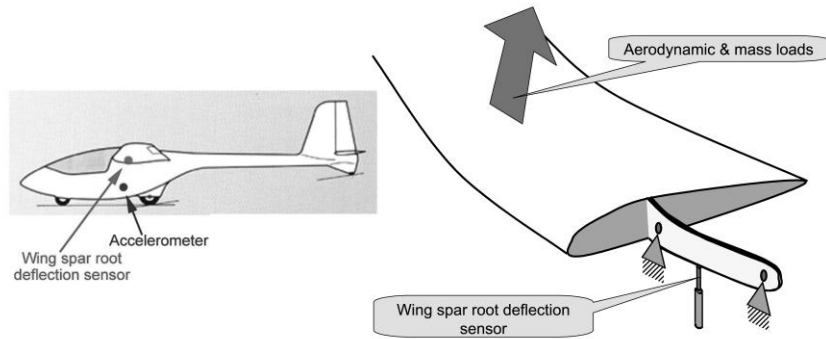


Figure 1 Basic system for load spectrum measuring.

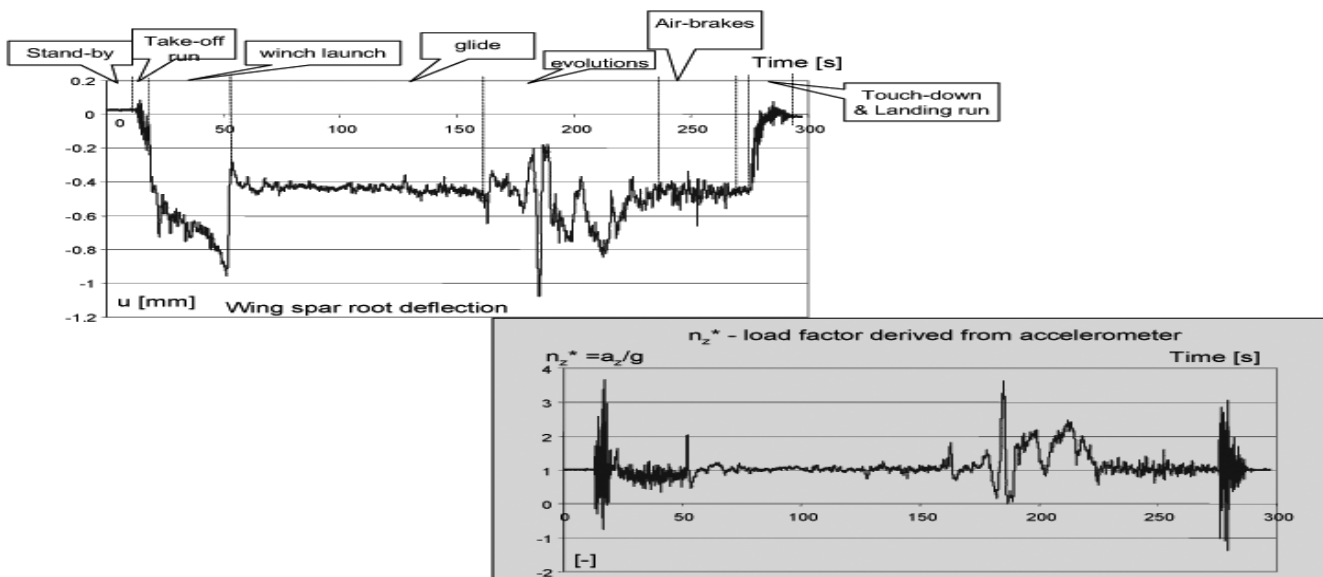


Figure 2 Sample time-courses of recorded signals.

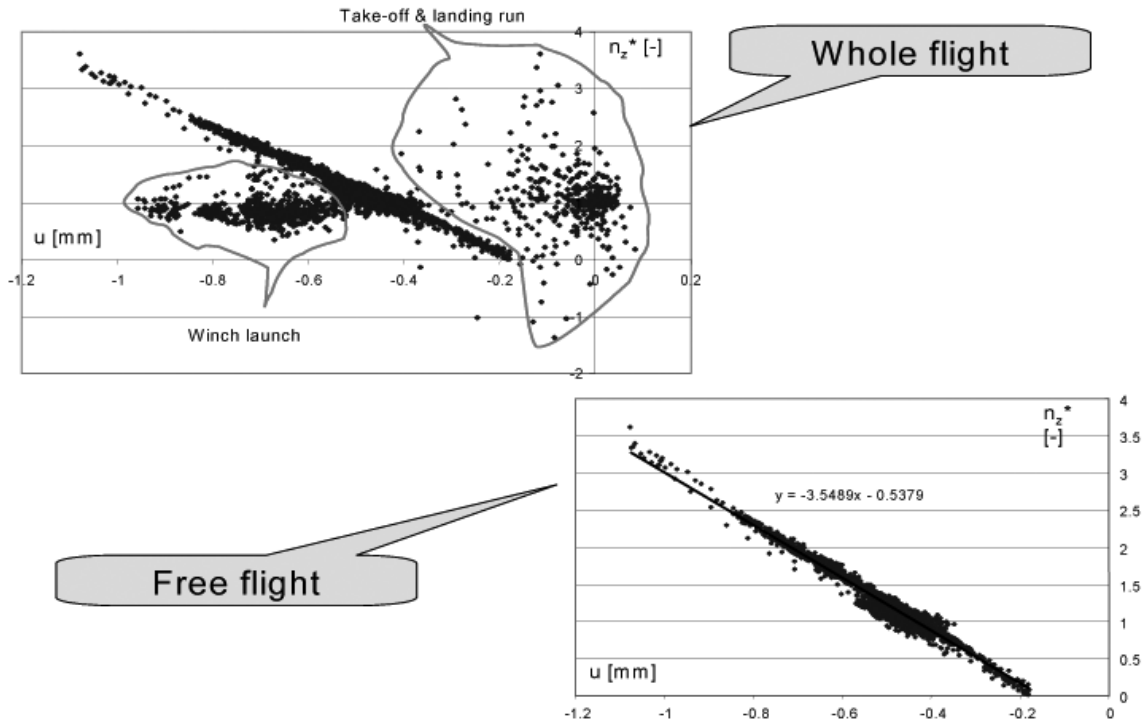


Figure 3 Correlation of the signals.

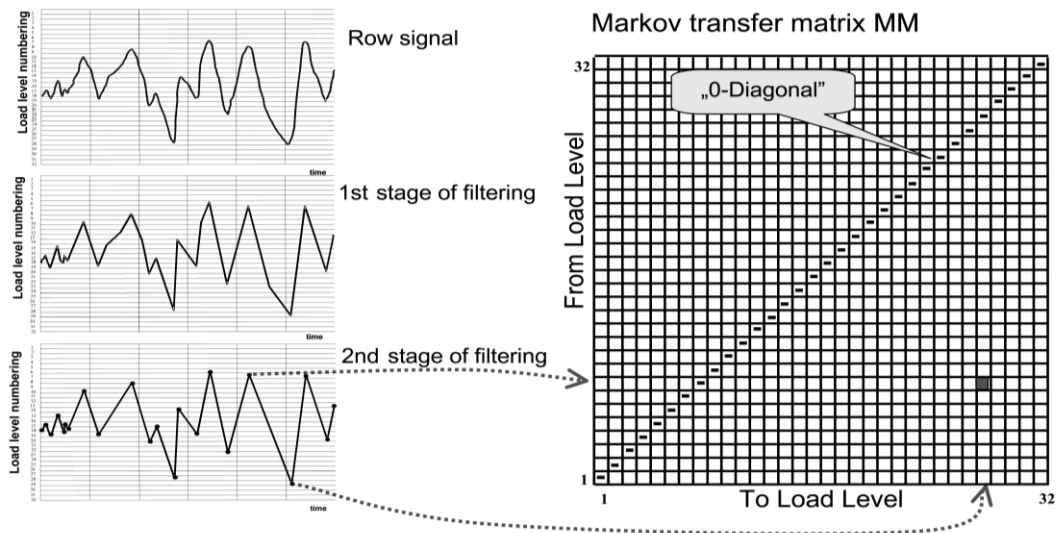


Figure 4 Recording the load signal in the Markov-matrix.

LL	1	2	3	4	5	6	7	8	9	10	11	12	13	14	15	16	17	18	19	20	21	22	23	24	25	26	27	28	29	30	31	32				
32																																				
31																																				
30																																				
29																																				
28																																				
27																																				
26																																				
25																																				
24																							5	74												
23																			1	1	3	8		74												
22																			1	3	8	5														
21									1						1			1	2		1	5														
20																	1	2	3		2	2														
19															1	1	9	108		2	1	1														
18															2	3	14		110	1																
17															4	11		15	7	1	1															
16																																				
15															2	10		11	2	2	1															
14														1	6		12	4	1																	
13													4		7			1																		
12													4								1															
11																							1													
10																																				
9																																				
8																																				
7																																				
6																																				
5																																				
4																																				
3																																				
2																																				
1																																				

Figure 5 Markov Matrix derived from the recorded signal.

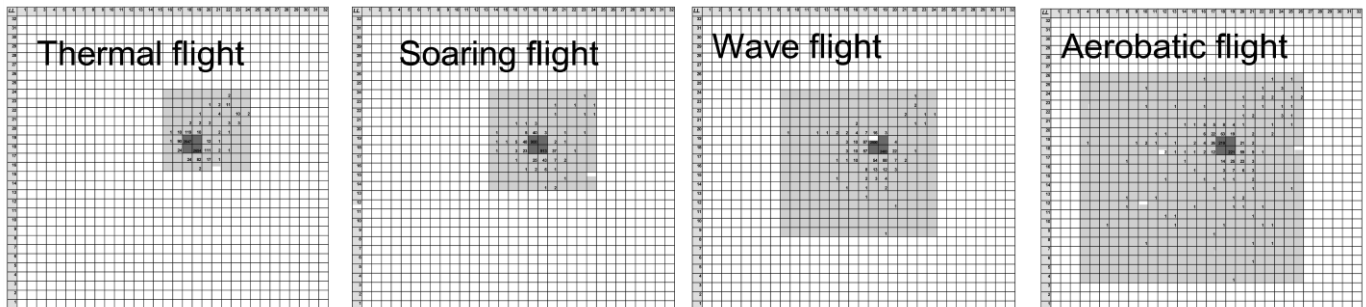


Figure 6 Examples of the LSs.

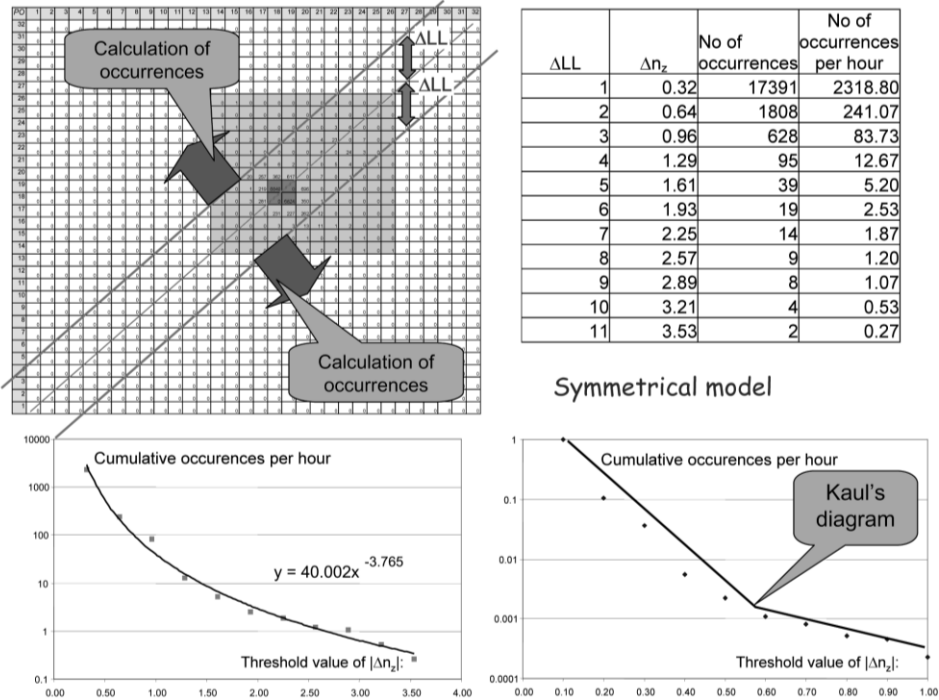


Figure 7 Incremental types of LS derived from MM (symmetrical concept).

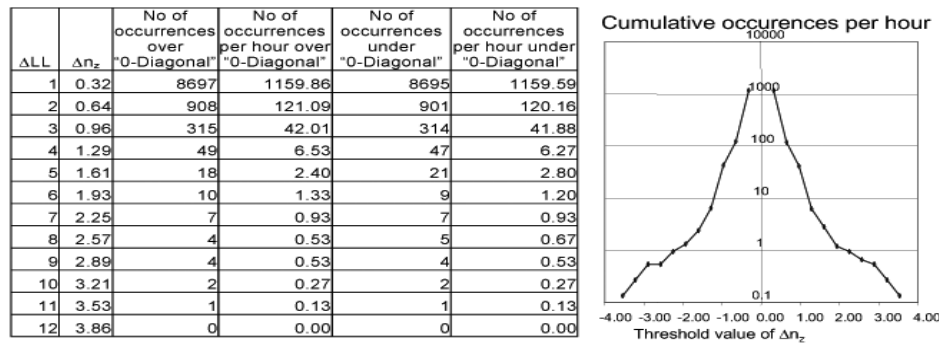


Figure 8 Incremental types of LS derived from MM (asymmetrical concept).

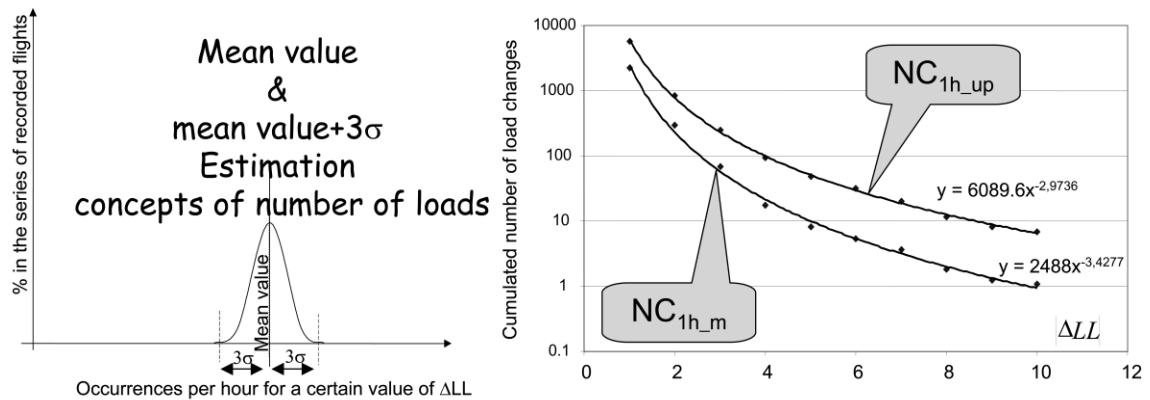


Figure 9 Analysis of occurrences for given ΔLL values

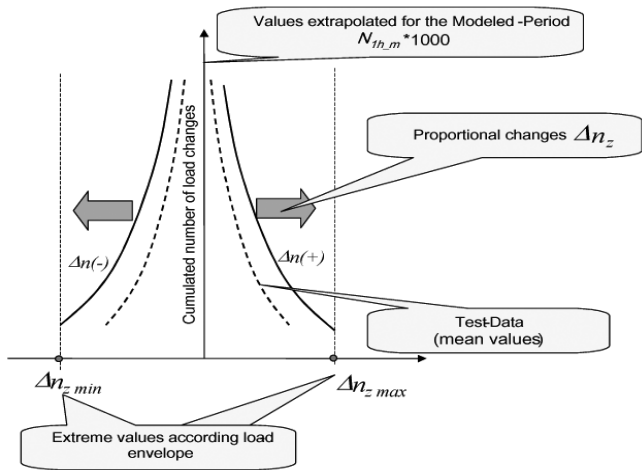


Figure 10 Method I – extrapolation by Test-Data range rescaling.

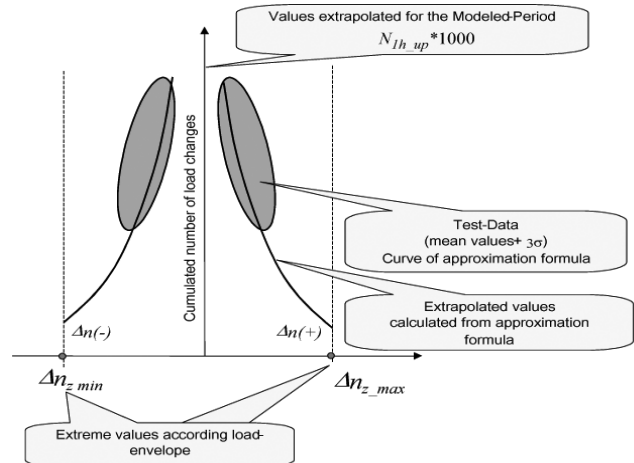


Figure 11 Method II – extrapolation by the “Test-Data + 3σ” approximation formula.

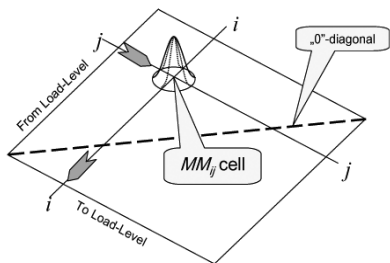


Figure 12 Idea of stochastic extrapolation.

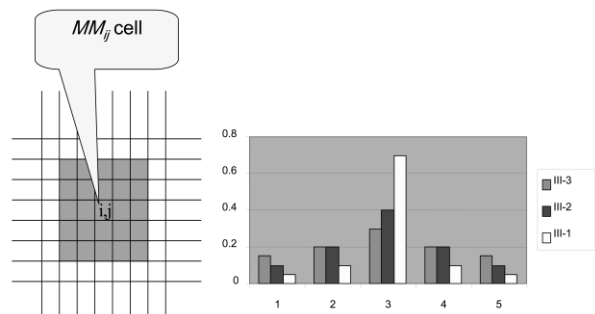


Figure 13 Probability distribution assumed in the program for the MM cell-values redistribution.

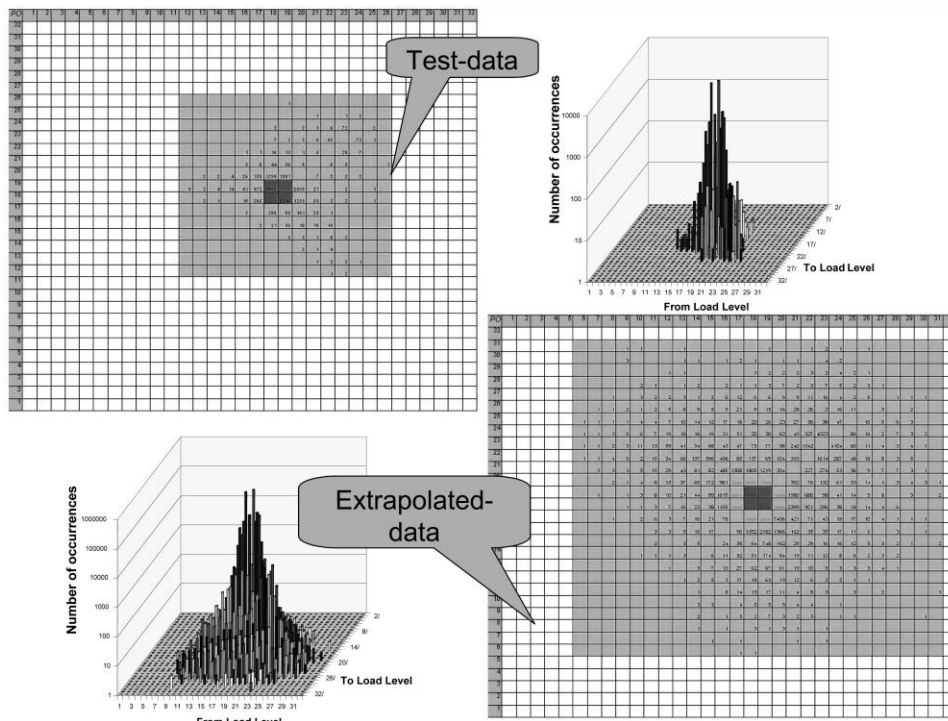


Figure 14 Result of stochastic extrapolation.

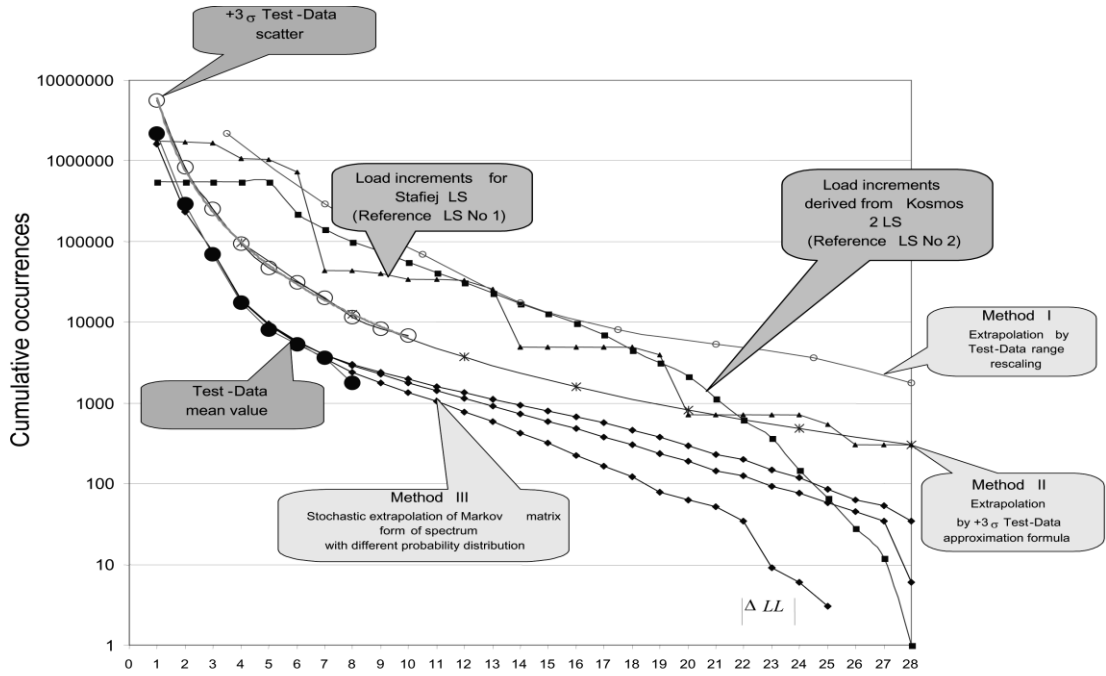


Figure 15 Comparison between the extrapolated LSs - cumulative number of occurrences aspect.

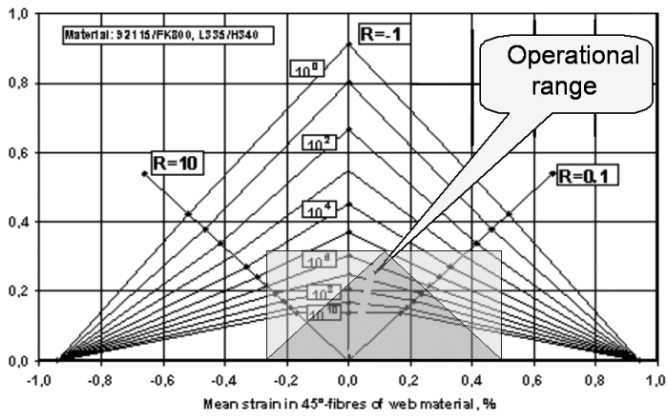


Figure 16 High diagram used for fatigue damage calculations.

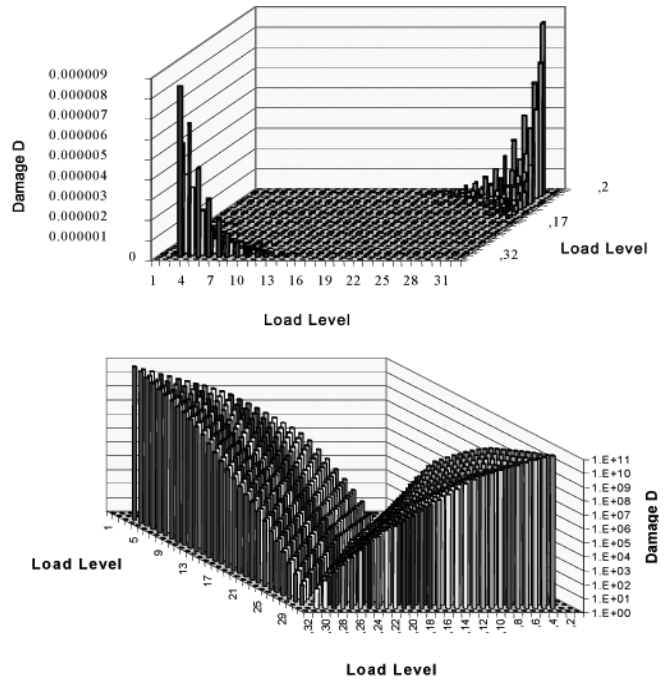


Figure 17 Array of elementary fatigue damages (effect of the unitary MM and the High diagram).

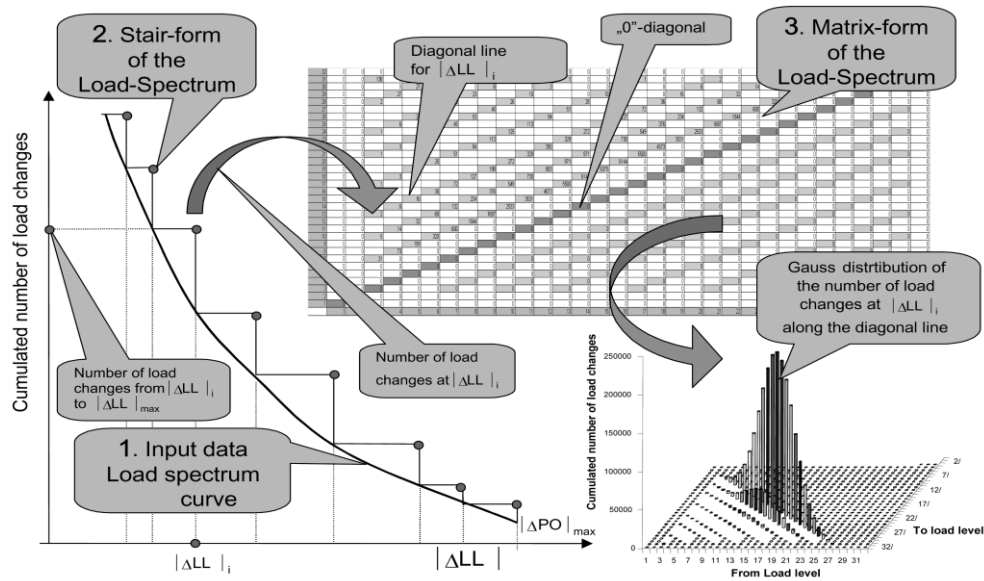


Figure 18 Algorithm of incremental LS to Markov-matrix transition.

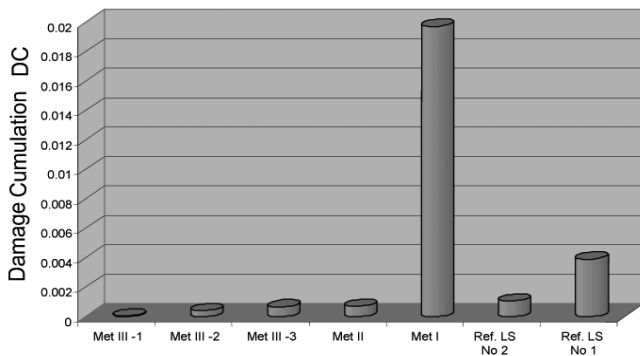


Figure 19 Comparison of extrapolated LSs - damage accumulation aspect.

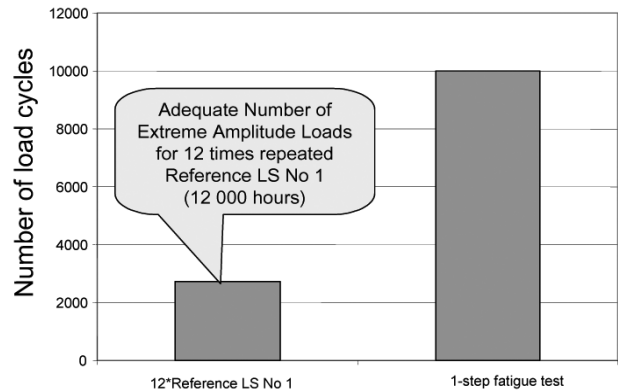


Figure 21 Substitution of the LS by Extreme-Amplitude Loads.

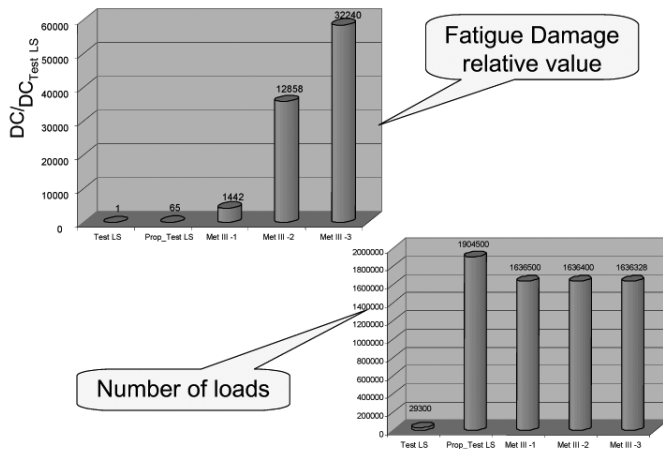


Figure 20 Fatigue damage and number of load changes.

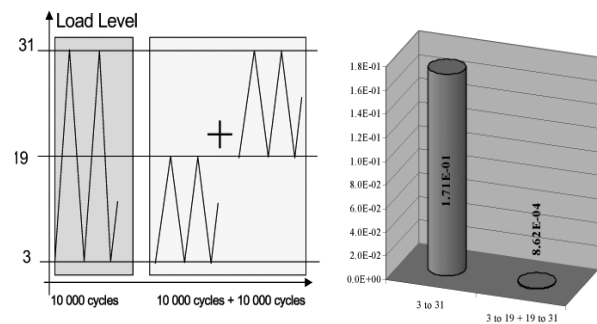


Figure 22 Comparison of damage accumulation for alternative load-profiles.